6.5 FIRST-ORDER AND SECOND-ORDER CONTINUOUS-TIME SYSTEMS

LTI systems described by linear constant-coefficient differential equations are of great practical importance, because many physical systems can be modeled by such equations and because systems of this type can often be conveniently implemented. For a variety of practical reasons, high-order systems are frequently implemented or represented by combining first-order and second-order systems in cascade or parallel arrangements. Consequently, the properties of first- and second-order systems play an important role in analyzing, designing, and understanding the time-domain and frequency-domain behavior of higher order systems. In this section, we discuss these low-order systems in detail for continuous time. In Section 6.6, we examine their discrete-time counterparts.

6.5.1 First-Order Continuous-Time Systems

The differential equation for a first-order system is often expressed in the form

$$\tau \frac{dy(t)}{dt} + y(t) = x(t), \tag{6.21}$$

where τ is a coefficient whose significance will be made clear shortly. The corresponding frequency response for the first-order system is

$$H(j\omega) = \frac{1}{j\omega\tau + 1}, \tag{6.22}$$

and the impulse response is

$$h(t) = \frac{1}{\tau} e^{-t/\tau} u(t), \tag{6.23}$$

which is sketched in Figure 6.19(a). The step response of the system is

$$s(t) = h(t) * u(t) = [1 - e^{-t/\tau}]u(t). \tag{6.24}$$

This is sketched in Figure 6.19(b). The parameter τ is the *time constant* of the system, and it controls the rate at which the first-order system responds. For example, as illustrated in Figure 6.19, at $t = \tau$ the impulse response has reached $1/e$ times its value at $t = 0$, and the step response is within $1/e$ of its final value. Therefore, as τ is decreased, the impulse response decays more sharply, and the rise time of the step response becomes shorter— i.e., it rises more sharply toward its final value. Note also that the step response of a first-order system does not exhibit any ringing.

Figure 6.20 depicts the Bode plot of the frequency response of eq. (6.22). In this figure we illustrate one of the advantages of using a logarithmic frequency scale: We can, without too much difficulty, obtain a useful approximate Bode plot for a continuous-time first-order system. To see this, let us first examine the plot of the log magnitude of the frequency response. Specifically, from eq. (6.22), we obtain

$$20\log_{10}|H(j\omega)| = -10\log_{10}[(\omega\tau)^2 + 1]. \tag{6.25}$$

From this, we see that for $\omega\tau \ll 1$, the log magnitude is approximately zero, while for $\omega\tau \gg 1$, the log magnitude is approximately a *linear* function of $\log_{10}(\omega)$. That is,

$$20\log_{10}|H(j\omega)| \simeq 0 \quad \text{for} \quad \omega \ll 1/\tau, \tag{6.26}$$

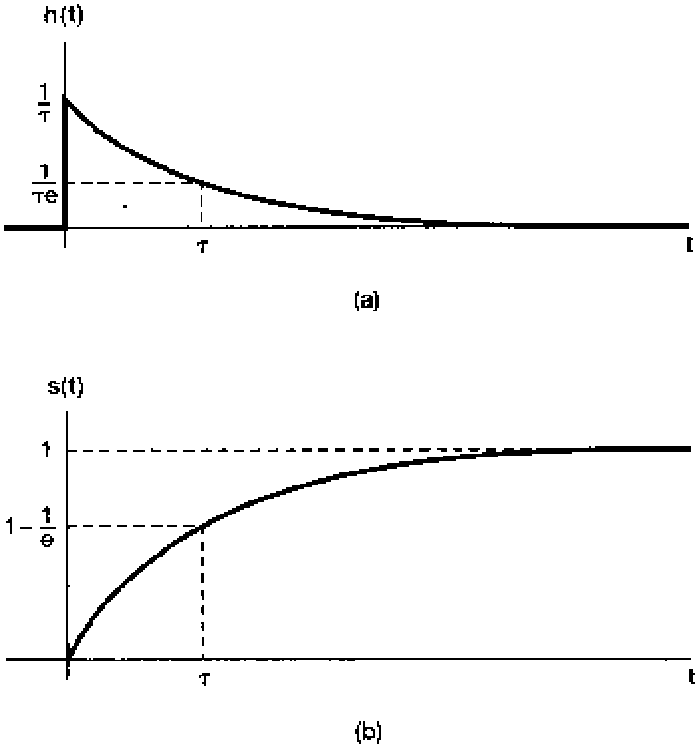

Figure 6.19 Continuous-time first-order system: (a) impulse response; (b) step response.

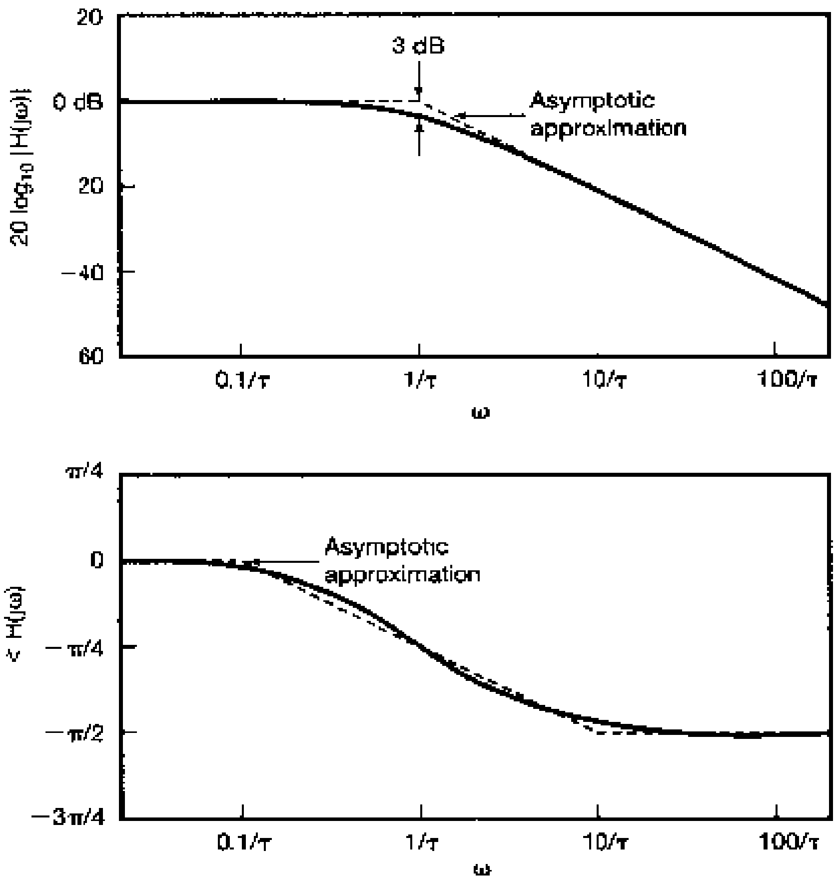

Figure 6.20 Bode plot for a continuous-time first-order system.

and

$$\begin{aligned} 20\log_{10}|H(j\omega)| &= -20\log_{10}(\omega\tau) \\ &= -20\log_{10}(\omega) - 20\log_{10}(\tau) \quad \text{for} \quad \omega \gg 1/\tau. \end{aligned} \tag{6.27}$$

In other words, for the first-order system, the low- and high-frequency asymptotes of the log magnitude are straight lines. The low-frequency asymptote [given by eq. (6.26)] is just the 0-dB line, while the high-frequency asymptote [specified by eq. (6.27)] corresponds to a decrease of 20 dB in $|H(j\omega)|$ for every decade (i.e., factor of 10) in ω. This is sometimes referred to as a "20-dB-per-decade" asymptote.

Note that the two asymptotic approximations given in eqs. (6.26) and (6.27) are equal at the point $\log_{10}(\omega) = -\log_{10}(\tau)$, or equivalently, $\omega = 1/\tau$. Interpreted graphically, this means that the two straight-line asymptotes meet at $\omega = 1/\tau$, which suggests a straight-line approximation to the magnitude plot. That is, our approximation to $20\log_{10}|H(j\omega)|$ equals 0 for $\omega \leq 1/\tau$ and is given by eq. (6.27) for $\omega \geq 1/\tau$. This approximation is also sketched (as a dashed line) in Figure 6.20. The point at which the slope of the approximation changes is precisely $\omega = 1/\tau$, which, for this reason, is often referred to as the *break frequency*. Also, note that at $\omega = 1/\tau$ the two terms $[(\omega\tau)^2$ and $1]$ in the argument of the logarithm in eq. (6.25) are equal. Thus, at this point, the actual value of the magnitude is

$$20\log_{10}\left|H\left(j\frac{1}{\tau}\right)\right| = -10\log_{10}(2) \simeq -3\text{ dB} \tag{6.28}$$

Because of this, the point $\omega = 1/\tau$ is sometimes called the 3-dB point. From the figure, we see that only near the break frequency is there any significant error in the straight-line approximate Bode plot. Thus, if we wish to obtain a more accurate sketch of the Bode plot, we need only modify the approximation near the break frequency.

It is also possible to obtain a useful straight-line approximation to $\sphericalangle H(j\omega)$:

$$\begin{aligned} \sphericalangle H(j\omega) &= -\tan^{-1}(\omega\tau) \\ &\simeq \begin{cases} 0, & \omega \leq 0.1/\tau \\ -(\pi/4)[\log_{10}(\omega\tau) + 1], & 0.1/\tau \leq \omega \leq 10/\tau. \\ -\pi/2, & \omega \geq 10/\tau \end{cases} \end{aligned} \tag{6.29}$$

Note that this approximation decreases linearly (from 0 to $-\pi/2$) as a function of $\log_{10}(\omega)$ in the range

$$\frac{0.1}{\tau} \leq \omega \leq \frac{10}{\tau},$$

i.e., in the range from one decade below the break frequency to one decade above the break frequency. Also, zero is the correct asymptotic value of $\sphericalangle H(j\omega)$ for $\omega \ll 1/\tau$, and $-\pi/2$ is the correct asymptotic value of $\sphericalangle H(j\omega)$ for $\omega \gg 1/\tau$. Furthermore, the approximation agrees with the actual value of $\sphericalangle H(j\omega)$ at the break frequency $\omega = 1/\tau$, at which point

$$\sphericalangle H\left(j\frac{1}{\tau}\right) = -\frac{\pi}{4}. \tag{6.30}$$

This asymptotic approximation is also plotted in Figure 6.20, and from it we can see how, if desired, we can modify the straight-line approximation to obtain a more accurate sketch of $\sphericalangle H(j\omega)$.

From this first-order system, we can again see the inverse relationship between time and frequency. As we make τ smaller, we speed up the time response of the system [i.e., $h(t)$ becomes more compressed toward the origin, and the rise time of the step response is reduced] and we simultaneously make the break frequency large [i.e., $H(j\omega)$ becomes broader, since $|H(j\omega)| \approx 1$ for a larger range of frequencies]. This can also be seen by multiplying the impulse response by τ and observing the relationship between $\tau h(t)$ and $H(j\omega)$:

$$\tau h(t) = e^{-t/\tau}u(t), \quad H(j\omega) = \frac{1}{j\omega\tau + 1}.$$

Thus, $\tau h(t)$ is a function of t/τ and $H(j\omega)$ is a function of $\omega\tau$, and from this we see that changing τ is essentially equivalent to a scaling in time and frequency.

6.5.2 Second-Order Continuous-Time Systems

The linear constant-coefficient differential equation for a second-order system is

$$\frac{d^2y(t)}{dt^2} + 2\zeta\omega_n\frac{dy(t)}{dt} + \omega_n^2 y(t) = \omega_n^2 x(t). \tag{6.31}$$

Equations of this type arise in many physical systems, including RLC circuits and mechanical systems, such as the one illustrated in Figure 6.21, composed of a spring, a mass, and a viscous damper or dashpot. In the figure, the input is the applied force $x(t)$ and the output is the displacement of the mass $y(t)$ from some equilibrium position at which the spring exerts no restoring force. The equation of motion for this system is

$$m\frac{d^2y(t)}{dt^2} = x(t) - ky(t) - b\frac{dy(t)}{dt},$$

or

$$\frac{d^2y(t)}{dt^2} + \left(\frac{b}{m}\right)\frac{dy(t)}{dt} + \left(\frac{k}{m}\right)y(t) = \frac{1}{m}x(t).$$

Comparing this to eq. (6.31), we see that if we identify

$$\omega_n = \sqrt{\frac{k}{m}} \tag{6.32}$$

and

$$\zeta = \frac{b}{2\sqrt{km}},$$

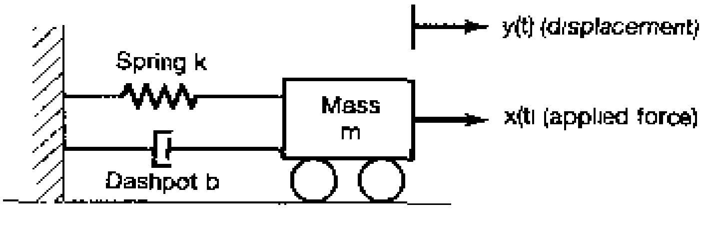

Figure 6.21 Second-order system consisting of a spring and dashpot attached to a moveable mass and a fixed support.

then [except for a scale factor of k on $x(t)$] the equation of motion for the system of Figure 6.21 reduces to eq. (6.31).

The frequency response for the second-order system of eq. (6.31) is

$$H(j\omega) = \frac{\omega_n^2}{(j\omega)^2 + 2\zeta\omega_n(j\omega) + \omega_n^2}. \tag{6.33}$$

The denominator of $H(j\omega)$ can be factored to yield

$$H(j\omega) = \frac{\omega_n^2}{(j\omega - c_1)(j\omega - c_2)},$$

where

$$\begin{aligned} c_1 &= -\zeta\omega_n + \omega_n\sqrt{\zeta^2 - 1}, \\ c_2 &= -\zeta\omega_n - \omega_n\sqrt{\zeta^2 - 1}. \end{aligned} \tag{6.34}$$

For $\zeta \neq 1$, c_1 and c_2 are unequal, and we can perform a partial-fraction expansion of the form

$$H(j\omega) = \frac{M}{j\omega - c_1} - \frac{M}{j\omega - c_2}, \tag{6.35}$$

where

$$M = \frac{\omega_n}{2\sqrt{\zeta^2 - 1}}. \tag{6.36}$$

From eq. (6.35), the corresponding impulse response for the system is

$$h(t) = M[e^{c_1 t} - e^{c_2 t}]u(t). \tag{6.37}$$

If $\zeta = 1$, then $c_1 = c_2 = -\omega_n$, and

$$H(j\omega) = \frac{\omega_n^2}{(j\omega + \omega_n)^2}. \tag{6.38}$$

From Table 4.2, we find that in this case the impulse response is

$$h(t) = \omega_n^2 t e^{-\omega_n t} u(t). \tag{6.39}$$

Note from eqs. (6.37) and (6.39), that $h(t)/\omega_n$ is a function of $\omega_n t$. Furthermore, eq. (6.33) can be rewritten as

$$H(j\omega) = \frac{1}{(j\omega/\omega_n)^2 + 2\zeta(j\omega/\omega_n) + 1},$$

from which we see that the frequency response is a function of ω/ω_n. Thus, changing ω_n is essentially identical to a time and frequency scaling.

The parameter ζ is referred to as the *damping ratio* and the parameter ω_n as the *undamped natural frequency*. The motivation for this terminology becomes clear when we take a more detailed look at the impulse response and the step response of a second-order system. First, from eq. (6.35), we see that for $0 < \zeta < 1$, c_1 and c_2 are complex, and we can rewrite the impulse response in eq. (6.37) in the form

$$\begin{aligned} h(t) &= \frac{\omega_n e^{-\zeta\omega_n t}}{2j\sqrt{1-\zeta^2}}\{\exp[j(\omega_n\sqrt{1-\zeta^2})t] - \exp[-j(\omega_n\sqrt{1-\zeta^2})t]\}u(t) \\ &= \frac{\omega_n e^{-\zeta\omega_n t}}{\sqrt{1-\zeta^2}}[\sin(\omega_n\sqrt{1-\zeta^2})t]u(t). \end{aligned} \tag{6.40}$$

Thus, for $0 < \zeta < 1$, the second-order system has an impulse response that has damped oscillatory behavior, and in this case the system is referred to as being *underdamped*. If $\zeta > 1$, both c_1 and c_2 are real and negative, and the impulse response is the difference between two decaying exponentials. In this case, the system is *overdamped*. The case of $\zeta = 1$, when $c_1 = c_2$, is called the *critically damped* case. The impulse responses (multiplied by $1/\omega_n$) for second-order systems with different values of ζ are plotted in Figure 6.22(a).

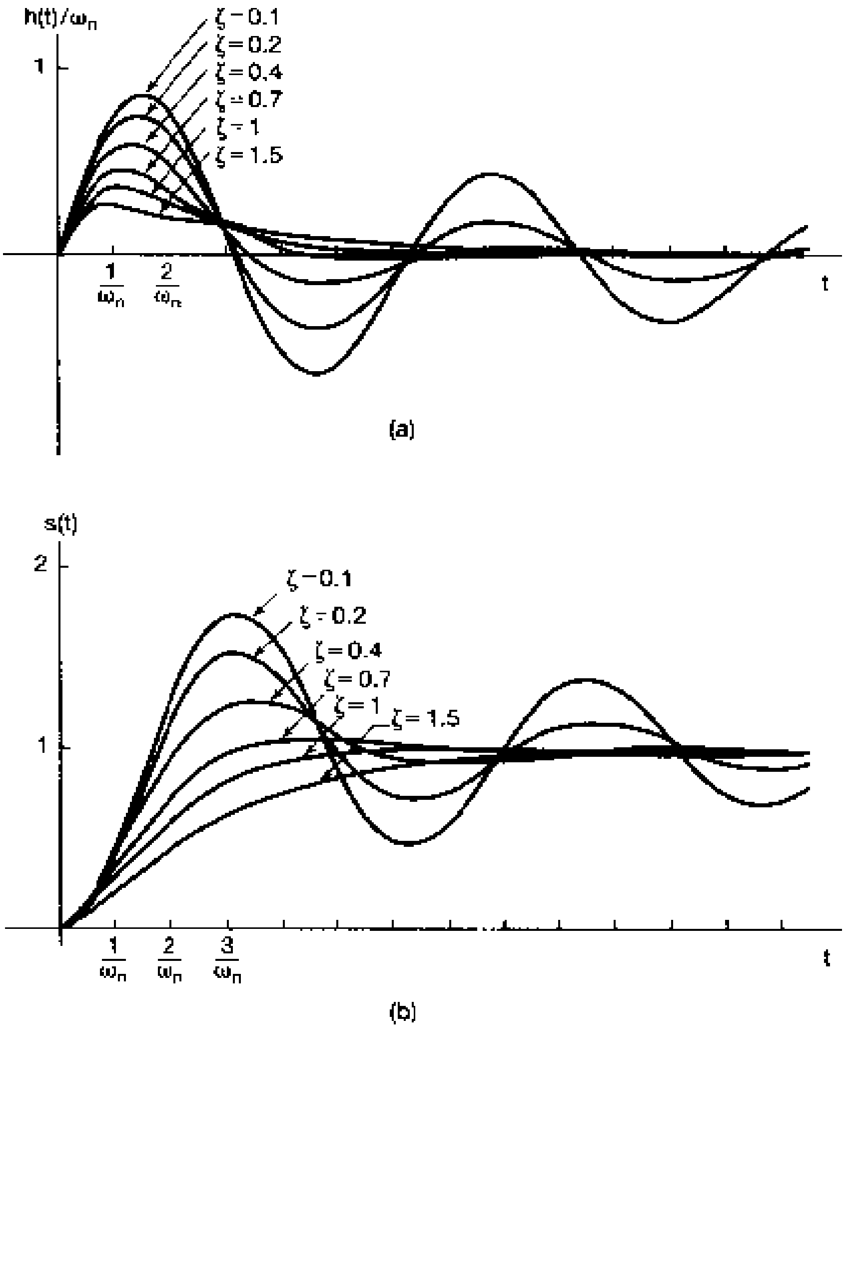

Figure 6.22 Response of continuous-time second-order systems with different values of the damping ratio ζ: (a) impulse response; (b) step response

The step response of a second-order system can be calculated from eq. (6.37) for $\zeta \neq 1$. This yields the expression

$$s(t) = h(t) * u(t) = \left\{1 + M\left[\frac{e^{c_1 t}}{c_1} - \frac{e^{c_2 t}}{c_2}\right]\right\} u(t). \tag{6.41}$$

For $\zeta = 1$, we can use eq. (6.39) to obtain

$$s(t) = [1 - e^{-\omega_n t} - \omega_n t e^{-\omega_n t}]u(t). \tag{6.42}$$

The step response of a second-order system is plotted in Figure 6.22(b) for several values of ζ. From this figure, we see that in the underdamped case, the step response exhibits both *overshoot* (i.e., the step response exceeds its final value) and *ringing* (i.e., oscillatory behavior). For $\zeta = 1$, the step response has the fastest response (i.e., the shortest rise time) that is possible without overshoot and thus has the shortest settling time. As ζ increases beyond 1, the response becomes slower. This can be seen from eqs. (6.34) and (6.41). As ζ increases, c_1 becomes smaller in magnitude, while c_2 increases in magnitude. Therefore, although the time constant ($1/|c_2|$) associated with $e^{c_2 t}$ decreases, the time constant ($1/|c_1|$) associated with $e^{c_1 t}$ increases. Consequently the term involving $e^{c_1 t}$ in eq. (6.41) takes a longer time to decay to zero, and thus it is the time constant associated with this term that determines the settling time of the step response. As a result the step response takes longer to settle for large values of ζ. In terms of our spring-dashpot example, as we increase the magnitude of the damping coefficient b beyond the critical value at which ζ in eq. (6.33) equals 1, the motion of the mass becomes increasingly sluggish.

Finally, note that, as we have said, the value of ω_n essentially controls the time scale of the responses $h(t)$ and $s(t)$. For example, in the underdamped case, the larger ω_n is, the more compressed is the impulse response as a function of t, and the higher is the frequency of the oscillations or ringing in both $h(t)$ and $s(t)$. In fact, from eq. (6.40), we see that the frequency of the oscillations in $h(t)$ and $s(t)$ is $\omega_n\sqrt{1-\zeta^2}$, which does increase with increasing ω_n. Note, however, that this frequency depends explicitly on the damping ratio and does not equal (and is in fact smaller than) ω_n, except in the *undamped* case, $\zeta = 0$. (It is for this reason that the parameter ω_n is traditionally referred to as the undamped natural frequency.) For the spring-dashpot example, we therefore conclude that the rate of oscillation of the mass equals ω_n when no dashpot is present, and the oscillation frequency decreases when we include the dashpot.

In Figure 6.23, we have depicted the Bode plot of the frequency response given in eq. (6.33) for several values of ζ. As in the first-order case, the logarithmic frequency scale leads to linear high- and low-frequency asymptotes for the log magnitude. Specifically, from eq. (6.33),

$$20\log_{10}|H(j\omega)| = -10\log_{10}\left\{\left[1-\left(\frac{\omega}{\omega_n}\right)^2\right]^2 + 4\zeta^2\left(\frac{\omega}{\omega_n}\right)^2\right\}. \tag{6.43}$$

From this expression, it follows that

$$20\log_{10}|H(j\omega)| \simeq \begin{cases} 0, & \text{for } \omega \ll \omega_n \\ -40\log_{10}\omega + 40\log_{10}\omega_n, & \text{for } \omega \gg \omega_n \end{cases}. \tag{6.44}$$

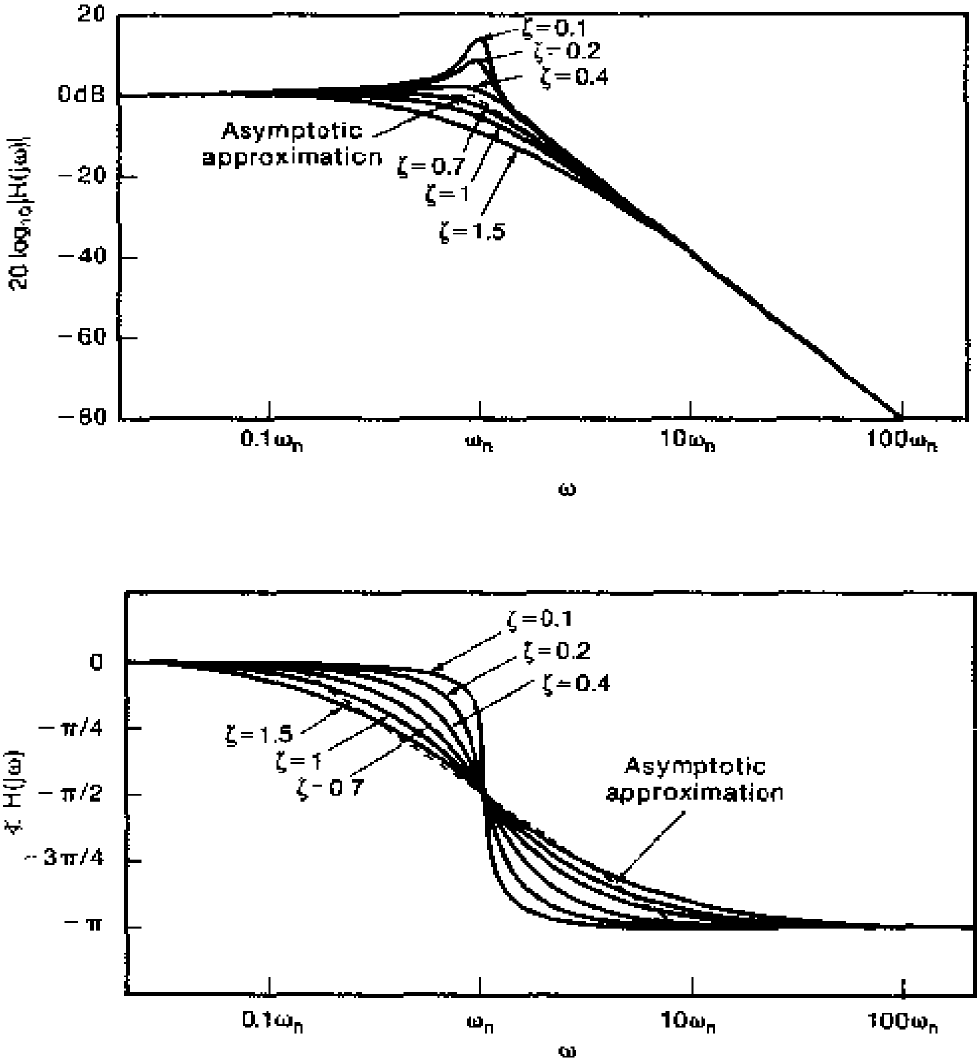

Figure 6.23 Bode plots for second-order systems with several different values of damping ratio ζ.

Therefore, the low-frequency asymptote of the log magnitude is the 0-dB line, while the high-frequency asymptote [given by eq. (6.44)] has a slope of -40 dB per decade; i.e., $|H(j\omega)|$ decreases by 40 dB for every increase in ω of a factor of 10. Also, note that the two straight-line asymptotes meet at the point $\omega = \omega_n$. Thus, we obtain a straight-line approximation to the log magnitude by using the approximation given in eq. (6.44) for $\omega \leq \omega_n$. For this reason, ω_n is referred to as the break frequency of the second-order system. This approximation is also plotted (as a dashed line) in Figure 6.23.

We can, in addition, obtain a straight-line approximation to $\sphericalangle H(j\omega)$, whose exact expression can be obtained from eq. (6.33):

$$\sphericalangle H(j\omega) = -\tan^{-1}\left(\frac{2\zeta(\omega/\omega_n)}{1-(\omega/\omega_n)^2}\right). \tag{6.45}$$

The approximation is

$$\sphericalangle H(j\omega) \approx \begin{cases} 0, & \omega \leq 0.1\omega_n \\ -\frac{\pi}{2}\left[\log_{10}\left(\frac{\omega}{\omega_n}\right) + 1\right], & 0.1\omega_n \leq \omega \leq 10\omega_n, \\ -\pi, & \omega \geq 10\omega_n \end{cases} \tag{6.46}$$

which is also plotted in Figure 6.23. Note that the approximation and the actual value again are equal at the break frequency $\omega = \omega_n$, where

$$\sphericalangle H(j\omega_n) = -\frac{\pi}{2}.$$

It is important to observe that the asymptotic approximations, eqs. (6.44) and (6.46), we have obtained for a second-order system do not depend on ζ, while the actual plots of $|H(j\omega)|$ and $\sphericalangle H(j\omega)$ certainly do, and thus, to obtain an accurate sketch, especially near the break frequency $\omega = \omega_n$, we must take this into account by modifying the approximations to conform more closely to the actual plots. The discrepancy is most pronounced for small values of ζ. In particular, note that in this case the actual log magnitude has a peak around $\omega = \omega_n$. In fact, straightforward calculations using eq. (6.43) show that, for $\zeta < \sqrt{2}/2 \approx 0.707$, $|H(j\omega)|$ has a maximum value at

$$\omega_{\max} = \omega_n\sqrt{1 - 2\zeta^2}, \tag{6.47}$$

and the value at this maximum point is

$$|H(j\omega_{\max})| = \frac{1}{2\zeta\sqrt{1-\zeta^2}}. \tag{6.48}$$

For $\zeta > 0.707$, however, $H(j\omega)$ decreases monotonically as ω increases from zero. The fact that $H(j\omega)$ can have a peak is extremely important in the design of frequency-selective filters and amplifiers. In some applications, one may want to design such a circuit so that it has a sharp peak in the magnitude of its frequency response at some specified frequency, thereby providing large frequency-selective amplification for sinusoids at frequencies within a narrow band. The *quality* Q of such a circuit is defined to be a measure of the sharpness of the peak. For a second-order circuit described by an equation of the form of eq. (6.31), the quality is usually taken to be

$$Q = \frac{1}{2\zeta},$$

and from Figure 6.23 and eq. (6.48), we see that this definition has the proper behavior: The less damping there is in the system, the sharper is the peak in $|H(j\omega)|$.

6.5.3 Bode Plots for Rational Frequency Responses

At the start of this section, we indicated that first- and second-order systems can be used as basic building blocks for more complex LTI systems with rational frequency responses. One consequence of this is that the Bode plots presented here essentially provide us with all of the information we need to construct Bode plots for arbitrary rational frequency responses. Specifically, we have described the Bode plots for the frequency responses given by eqs. (6.22) and (6.33). In addition, we can readily obtain the Bode plots for frequency responses of the forms

$$H(j\omega) = 1 + j\omega\tau \tag{6.49}$$

and

$$H(j\omega) = 1 + 2\zeta\left(\frac{j\omega}{\omega_n}\right) + \left(\frac{j\omega}{\omega_n}\right)^2 \tag{6.50}$$

The Bode plots for eqs. (6.49) and (6.50) follow directly from Figures 6.20 and 6.23 and from the fact that

$$20\log_{10}|H(j\omega)| = -20\log_{10}\left|\frac{1}{H(j\omega)}\right|$$

and

$$\sphericalangle(H(j\omega)) = -\sphericalangle\left(\frac{1}{H(j\omega)}\right).$$

Also, consider a system function that is a constant gain

$$H(j\omega) = K.$$

Since $K = |K|e^{j\cdot 0}$ if $K > 0$ and $K = |K|e^{j\pi}$ if $K < 0$, we see that

$$20\log_{10}|H(j\omega)| = 20\log_{10}|K|$$

$$\sphericalangle H(j\omega) = \begin{cases} 0, & \text{if } K > 0 \\ \pi, & \text{if } K < 0 \end{cases}$$

Since a rational frequency response can be factored into the product of a constant gain and first- and second-order terms, its Bode plot can be obtained by summing the plots for each of the terms. We illustrate further the construction of Bode plots in the next two examples.

Example 6.4

Let us obtain the Bode plot for the frequency response

$$H(j\omega) = \frac{2 \times 10^4}{(j\omega)^2 + 100j\omega + 10^4}.$$

First, we note that

$$H(j\omega) = 2\hat{H}(j\omega),$$

where $\hat{H}(j\omega)$ has the same form as the standard second-order frequency response specified by eq. (6.33). It follows that

$$20\log_{10}|H(j\omega)| = 20\log_{10}2 + 20\log|\hat{H}(j\omega)|.$$

By comparing $\hat{H}(j\omega)$ with the frequency response in eq (6.33), we conclude that $\omega_n = 100$ and $\zeta = 1/2$ for $\hat{H}(j\omega)$. Using eq. (6.44), we may now specify the asymptotes for $20\log_{10}|\hat{H}(j\omega)|$:

$$20\log_{10}|\hat{H}(j\omega)| \simeq 0 \quad \text{for } \omega \ll 100,$$

and

$$20\log_{10}|\hat{H}(j\omega)| \simeq -40\log_{10}\omega + 80 \quad \text{for } \omega \gg 100.$$

It follows that $20\log_{10}|H(j\omega)|$ will have the same asymptotes, except for a constant offset at all frequencies due to the addition of the $20\log_{10}2$ term (which approximately equals 6 dB). The dashed lines in Figure 6.24(a) represent these asymptotes.

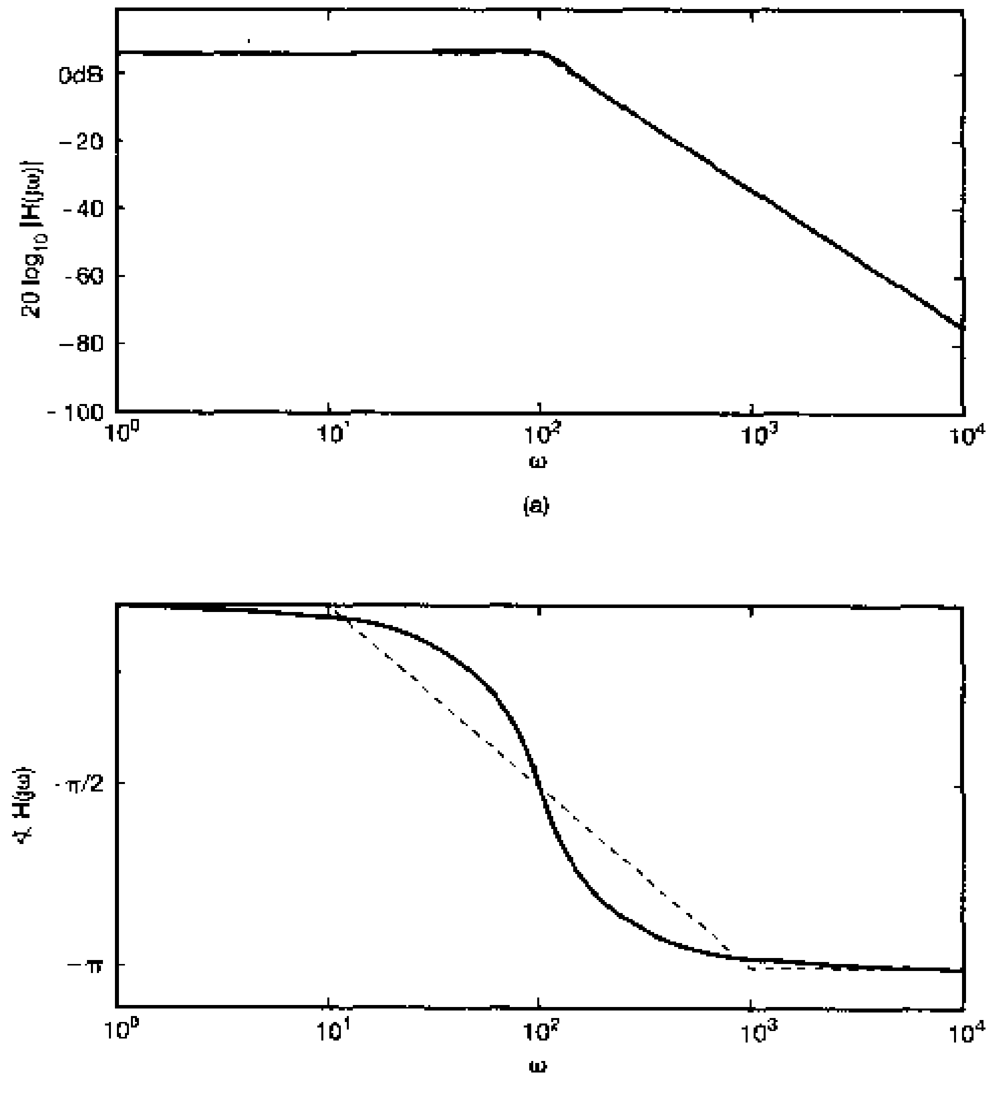

Figure 6.24 Bode plot for system function in Example 6.4. (a) magnitude, (b) phase

The solid curve in the same figure represents the actual computer-generated Bode plot for $20\log_{10}|H(j\omega)|$. Since the value of ζ for $\hat{H}(j\omega)$ is less than $\sqrt{2}/2$, the actual Bode plot has a slight peak near $\omega = 100$.

To obtain a plot of $\sphericalangle H(j\omega)$, we note that

$$\sphericalangle H(j\omega) = \sphericalangle \hat{H}(j\omega)$$

and that $\sphericalangle \hat{H}(j\omega)$ has its asymptotes specified in accordance with eq. (6.46); that is,

$$\sphericalangle \hat{H}(j\omega) = \begin{cases} 0, & \omega \le 10 \\ -(\pi/2)[\log_{10}(\omega/100) + 1], & 10 \le \omega \le 1{,}000. \\ -\pi, & \omega \ge 1{,}000. \end{cases}$$

The asymptotes and the actual values for $\sphericalangle H(j\omega)$ are plotted with dashed and solid lines, respectively, in Figure 6.24(b).

Example 6.5

Consider the frequency response

$$H(j\omega) = \frac{100(1 + j\omega)}{(10 + j\omega)(100 + j\omega)}$$

To obtain the Bode plot for $H(j\omega)$, we rewrite it in the following factored form:

$$H(j\omega) = \left(\frac{1}{10}\right)\left(\frac{1}{1 + j\omega/10}\right)\left(\frac{1}{1 + j\omega/100}\right)(1 + j\omega).$$

Here, the first factor is a constant, the next two factors have the standard form for a first-order frequency response as specified in eq. (6.22), and the fourth factor is the reciprocal of the same first-order standard form. The Bode plot for $20\log_{10}|H(j\omega)|$ is therefore the sum of the Bode plots corresponding to each of the factors. Furthermore, the asymptotes corresponding to each factor may be summed to obtain the asymptotes for the overall Bode plot. These asymptotes and the actual values of $20\log_{10}|H(j\omega)|$ are displayed in Figure 6.25(a). Note that the constant factor of 1/10 accounts for an offset of -20 dB at each frequency. The break frequency at $\omega = 1$ corresponds to the $(1 + j\omega)$ factor, which produces the 20 dB/decade rise that starts at $\omega = 1$ and is canceled by the 20 dB/decade decay that starts at the break frequency at $\omega = 10$ and is due to the $1/(1 + j\omega/10)$ factor. Finally, the $1/(1 + j\omega/100)$ factor contributes another break frequency at $\omega = 100$ and a subsequent decay at the rate of 20 dB/decade.

Similarly we can construct the asymptotic approximation for $H(j\omega)$ from the individual asymptotes for each factor, as illustrated, together with a plot of the exact value of the phase, in Figure 6.25(b). In particular, the constant factor 1/10 contributes 0 to the phase, while the factor $(1 + j\omega)$ contributes an asymptotic approximation that is 0 for $\omega < 0.1$, and rises linearly as a function of $\log_{10}(\omega)$ from a value of zero at $\omega = 0.1$ to a value of $\pi/2$ radians at $\omega = 10$. However, this rise is canceled at $\omega = 1$ by the asymptotic approximation for the angle of $1/(1 + j\omega/10)$ which contributes a linear decrease in angle of $\pi/2$ radians over the range of frequencies from $\omega = 1$ to $\omega = 100$. Finally, the asymptotic approximation for the angle of $1/(1 + j\omega/100)$ contributes another linear decrease in angle of $\pi/2$ radians over the range of frequencies from $\omega = 10$ to $\omega = 1000$.

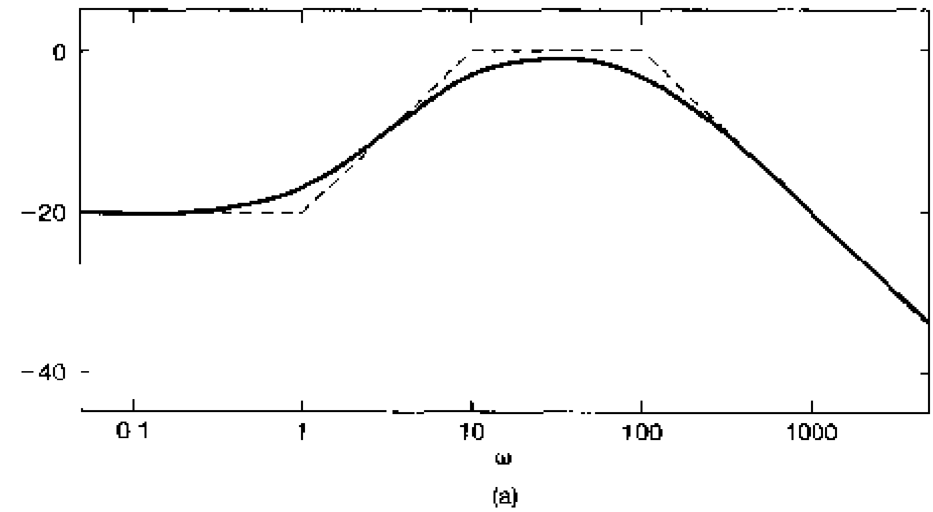

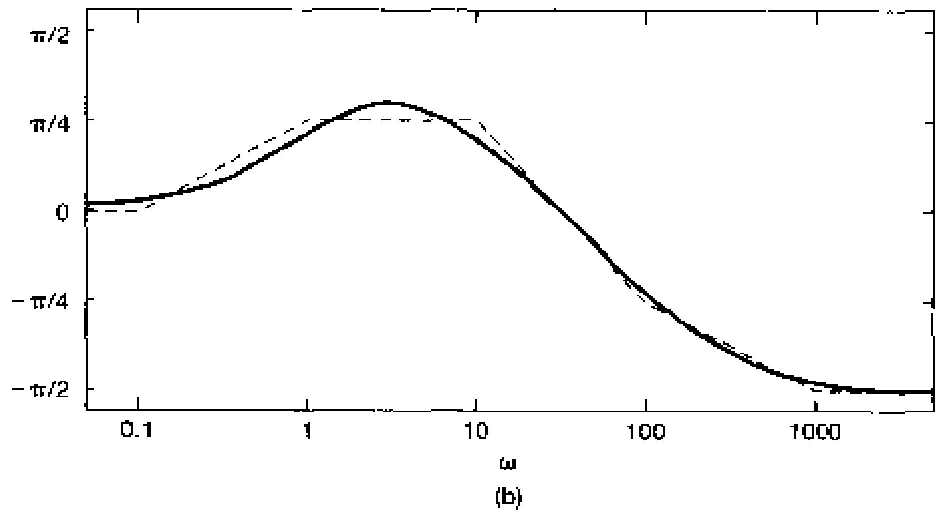

Figure 6.25 Bode plot for system function in Example 6.5: (a) magnitude; (b) phase.

In our discussion of first-order systems in this section, we restricted our attention to values of $\tau > 0$. In fact, it is not difficult to check that if $\tau < 0$, then the causal first-order system described by eq. (6.21) has an impulse response that is not absolutely integrable, and consequently, the system is unstable. Similarly, in analyzing the second-order causal system in eq. (6.31), we required that both ζ and ω_n^2 be positive numbers. If either of these is not positive, the resulting impulse response is not absolutely integrable. Thus, in this section we have restricted attention to those causal first- and second-order systems that are stable and for which we can define frequency responses.